Magn Reson Med Sci 2024; 23; 49–55
doi:10.2463/mrms.mp.2022-0082 Published Online: December 16, 2022

MAJOR PAPER

# Evaluating the Elasticity of Metastatic Cervical Lymph Nodes in Head and Neck Squamous Cell Carcinoma Patients Using DWI-based Virtual MR Elastography

Hye Na Jung[1], Inseon Ryoo[1*], Sangil Suh[1], Young Hen Lee[2], and Eunju Kim[3]

**Purpose:** The assessment of metastatic cervical lymph nodes in head and neck squamous cell carcinoma patients is crucial; as such, many studies focusing on non-invasive imaging techniques to evaluate metastatic cervical lymph nodes have been performed. The aim of our study was to assess the usefulness of elasticity values on diffusion weighted imaging (DWI)-based virtual MR elastography in the evaluation of metastatic cervical lymph nodes from head and neck squamous cell carcinoma.

**Methods:** Two head and neck radiologists measured the elasticity values of 16 metastatic cervical lymph nodes from head and neck squamous cell carcinoma and 13 benign cervical lymph nodes on DWI-based virtual MR elastography maps. Mean, minimum, maximum, and median elasticity values were evaluated for lymph nodes between the two groups and interobserver agreement in measuring the elasticity was also evaluated.

**Results:** The mean, maximum, and median elasticity values of metastatic cervical lymph nodes were significantly higher than those of benign cervical lymph nodes ($P$ = 0.001, 0.01, and 0.002, respectively). Diagnostic accuracy, sensitivity, and specificity of the mean elasticity were 82.8%, 93.8%, and 69.2%, respectively. Interobserver agreement was excellent for the mean and median elasticity (intraclass correlation coefficients were 0.98 for both).

**Conclusion:** Estimated elasticity values based on DWI-based virtual MR elastography show significant difference between benign and metastatic cervical lymph nodes from head and neck squamous cell carcinoma. While precise modulation of MR sequences and calibration parameters still needs to be established, elasticity values can be useful in differentiating between these lymph nodes.

**Keywords:** *diffusion-weighted image, virtual magnetic resonance imaging elastography, cervical lymph node, head and neck squamous cell carcinoma, metastasis*

## Introduction

Differentiation of metastatic cervical lymph nodes from benign cervical lymph nodes in head and neck squamous cell carcinoma (HNSCC) patients is crucial because it directly affects not only the prognosis but also the decision of treatment strategies.[1,2] Pathologic diagnosis is the gold-standard for the diagnosis of cervical lymph node disease; however, some patients with poor general condition such as coagulopathy cannot undergo tissue biopsy. In addition, some lymph nodes in certain anatomical locations including retropharyngeal nodes, deep intra-parotid nodes, or nodes located just posterior to the clavicles cannot be obtained through percutaneous biopsy. Besides the invasiveness, difficulties, and operator dependency of tissue biopsy, another problem in tissue biopsy is that only a limited portion of any lesion can be obtained through needle biopsy.[3]

Therefore, non-invasive imaging techniques for the assessment of metastatic cervical lymph nodes are desirable. However, differentiating between metastatic and benign cervical lymph nodes on cross-sectional imaging modalities such as ultrasound (US), CT, and MR imaging remains

[1]Department of Radiology, Korea University Guro Hospital, Korea University College of Medicine, Seoul, Korea
[2]Department of Radiology, Korea University Ansan Hospital, Korea University College of Medicine, Seoul, Korea
[3]Philips Healthcare Korea, Seoul, Korea

*Corresponding author: Department of Radiology, Korea University Guro Hospital, Korea University College of Medicine, 148, Gurodong-ro, Guro-gu, Seoul 08308, Korea. Phone: +82-2-2626-1339, Fax: +82-2-863-9282, E-mail: isryoo@gmail.com



Received: July 11, 2022 | Accepted: October 10, 2022

challenging when the evaluation is made on the basis of conventional morphological changes.[1,4–7]

Elasticity, an intrinsic tissue property, is how the tissue gets deformed under mechanical pressure. Malignant tumors have altered rigidity relative to normal tissue. Malignant lesions have greater cellularity, abundant extracellular matrix, and increased vascularity and interstitial pressure. These characteristics may result in increased tissue elasticity.[8–10] Many studies have reported that tissue elasticity is helpful in differentiating metastatic from benign cervical lymph nodes using US elastography.[11–14] On the other hand, MR elastography (MRE) may not be available in most institutions because it requires dedicated hardware and software, and lengthy imaging acquisition.[15,16] Recently, a strong correlation has been reported between tissue water diffusivity and elasticity in liver tissue. The shifted apparent diffusion coefficient (sADC) values were shown to be strongly correlated with tissue elasticity.[15–17] Another recent study showed the correlation between mean tissue elasticity on diffusion weighted imaging (DWI)-based virtual MRE and surgical consistency grading in pituitary adenomas.[18] These results suggest that DWI-based virtual MRE can be used to measure tissue elasticity.[17,18]

The purpose of this study was to assess tissue elasticity values in metastatic and benign cervical lymph nodes using DWI-based virtual MRE and to evaluate the usefulness of those values in differentiating metastatic from benign cervical lymph nodes in HNSCC patients. We also evaluated the interobserver agreement in the assessment of tissue elasticity values of cervical lymph nodes with DWI-based virtual MRE.

## Materials and Methods

This retrospective study was approved by the institutional review board of our institution and the need for informed consent was waived.

### *Study population*

A total of 61 patients underwent neck MR imaging including DWI-based virtual MRE between December 2021 and March 2022 in a university hospital. There were 47 patients with head and neck malignant tumors including two patients with lymphoma and one with mucoepidermoid carcinoma. Seven HNSCC patients without lymph node metastasis and 27 patients with a previous history of cancer treatment were excluded. All patients without malignant disease were included for benign cervical lymph nodes analysis. However, one patient without any discernible lymph nodes for drawing ROI was excluded. Finally, 10 patients with pathologically-proven cervical metastatic lymph nodes from HNSCC and 13 patients with benign cervical lymph nodes were included in this study.

### *MR imaging acquisition and analysis*

MR imaging was performed using a 3.0T MRI system (Elition X; Philips Healthcare, Best, the Netherlands) with a 32-channel dS head coil. DWI was performed using fat suppressed turbo spin-echo, single shot echo-planar sequence (SPLICE) with the following parameters: TR/TE, 3110/69 msec; FOV, 160 × 160 $mm^2$; matrix, 72 × 72; slice thickness, 3 mm; number of signal averages (NSA), 3; and average high b mode = yes (improve SNR of high b value DWI). An average of 30 contiguous sections was used. The turbo spin echo (TSE) factor was 34 and the total scan duration was 4 minutes.

The DWI scans were transferred to a workstation for analysis using virtual MRE analysis software (EXPRESS; Philips Healthcare Korea, Seoul, Korea). This software generated virtual MRE maps (virtual shear stiffness maps) and calculated sADC with two key b values of 200 and 1500 sec/$mm^2$ as used in previous studies as follows:[15–17]

$$\mathrm{sADC}\left(\mathrm{mm}^2/\mathrm{sec}\right) = \ln(S_{200}/S_{1500})/(1500-200),$$

where sADC is shifted ADC, $S_{200}$ is the image signal with a $b$ value of 200 sec/$mm^2$, and $S_{1500}$ is the image signal with a $b$ value of 1500 sec/$mm^2$. Diffusion-based virtual MRE maps were calculated as previously described:[16]

$$\mu_{\mathrm{Diff}}(\mathrm{kPa}) = \alpha \mathrm{sADC}\left(\mathrm{mm}^2/\mathrm{sec}\right) + \beta,$$

where $\mu_{\mathrm{Diff}}$ is diffusion-based shear modulus, sADC is shifted ADC, and the values for α and β were $-9.8 \pm 0.8$ and $14.0 \pm 0.9$, respectively.

The virtual MRE maps were generated on a voxel-by-voxel basis after removing the background signal while maintaining the head and neck soft tissue feature (Fig. 1).

After generation of the DWI-based virtual MRE maps, two head and neck neuro-radiologists (I.R. and H.N.J., both with 14 years of experience in this field) drew the ROIs. For metastatic cervical lymph nodes, the readers drew ROIs to include the entire region of each lymph node on the slice that showed the largest dimension of the lymph node (Figs. 1 and 2a). In the assessment of benign cervical lymph nodes, the readers selected the largest lymph node in each patient and drew ROIs to include the entire region of each node on the map (Fig. 3). The software generated several tissue elasticity indices including the mean, minimum, maximum, and median elasticity values with standard deviations in kilo-Pascal (kPa).

### *Statistical analysis*

The elasticity values, mean, minimum, maximum, and median elasticities on DWI-based virtual MRE of metastatic and benign cervical lymph nodes were compared using unpaired *t*-tests. The ability of elasticity values to differentiate between benign and metastatic cervical lymph nodes from HNSCC was evaluated by receiver operating characteristic (ROC) curve analysis. The optimal cutoff values for differentiating metastatic from benign cervical lymph nodes were identified by maximizing the Youden index. We also evaluated the accuracy, sensitivity, specificity, positive predictive value (PPV), and negative predictive value (NPV) with optimal cutoff values.

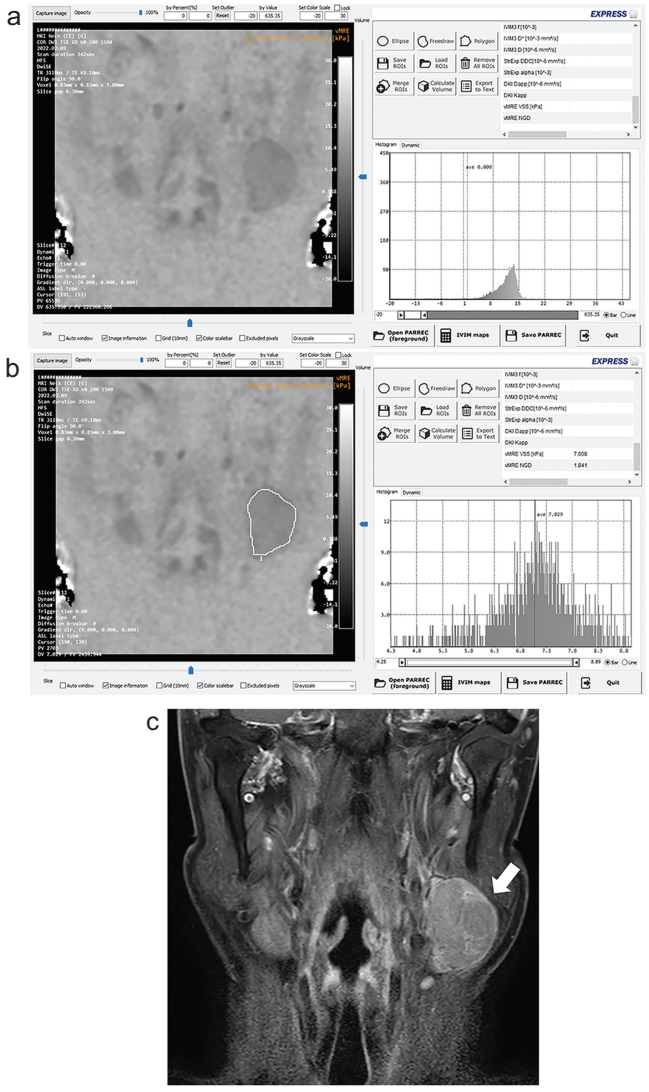


**Fig. 1** A 66-year-old male with left tonsillar squamous cell carcinoma with left level II lymph node metastasis. (**a**) DWI-based virtual MR elastography map is generated. (**b**) An ROI is placed on the metastatic lymph node to include the entire region of the node. (**c**) Contrast-enhanced coronal T1-weighted image shows the metastatic node (arrow). DWI, diffusion weighted imaging.

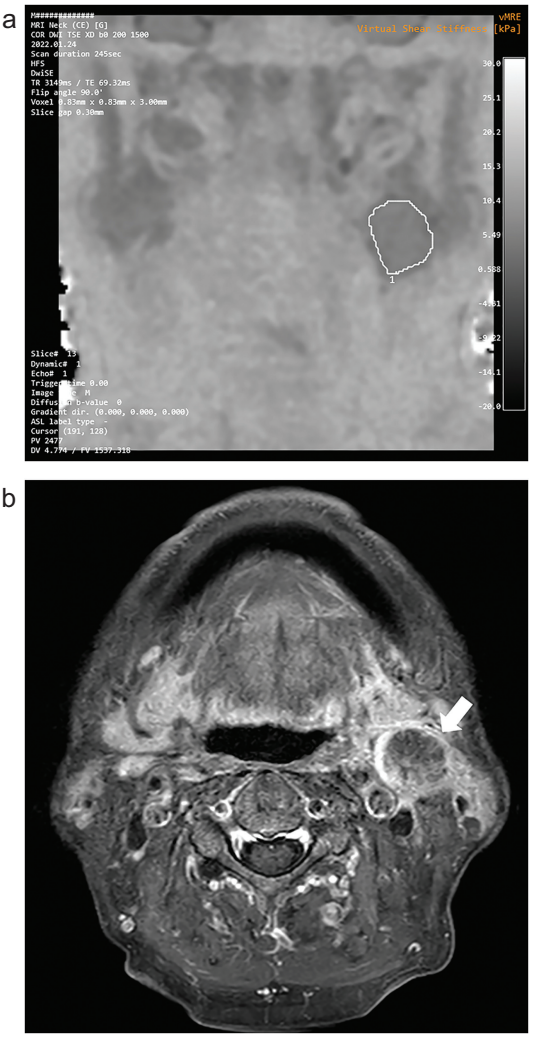


**Fig. 2** A 73-year-old male with left tonsillar squamous cell carcinoma with left level II lymph node metastasis. (**a**) An ROI is placed on the left level II metastatic lymph node to include the entire region of the node on the DWI-based virtual MR elastography map. (**b**) Contrast-enhanced, axial T1-weighted image shows severe internal necrosis of the lymph node (arrow). DWI, diffusion weighted imaging.

Interobserver agreement for measuring tissue elasticity values on DWI-based virtual MRE maps was evaluated by using intraclass correlation (ICC) (SPSS Version 18.0; SPSS, Chicago, IL, USA and MedCalc version 20.027; MedCalc Software, Mariakerke, Belgium). *P* values < 0.05 were considered statistically significant.

## Results

### *Patient characteristics*

We included 16 metastatic cervical lymph nodes from 10 HNSCC patients (M:F = 8:2; mean age, 67.6 ± 10.9 years; range, 52–83 years). All the metastatic lymph nodes were pathologically confirmed by core needle biopsy or surgery. Seven of these patients were diagnosed with oropharynx cancer, one patient with nasopharynx cancer, one patient with oral cavity cancer, and one with glottis cancer. A total of 13 benign cervical lymph nodes from 13 patients were included in the study (M:F = 8:5; mean age, 55.9 ± 19 years; range, 31–85 years). Ten patients were diagnosed with benign salivary gland tumors (four Warthin tumors, five pleomorphic adenomas, and one basal cell adenoma, all in the parotid glands), one patient with neurogenic tumor, one with giant cell granuloma, and one without any pathologic findings (Table 1).

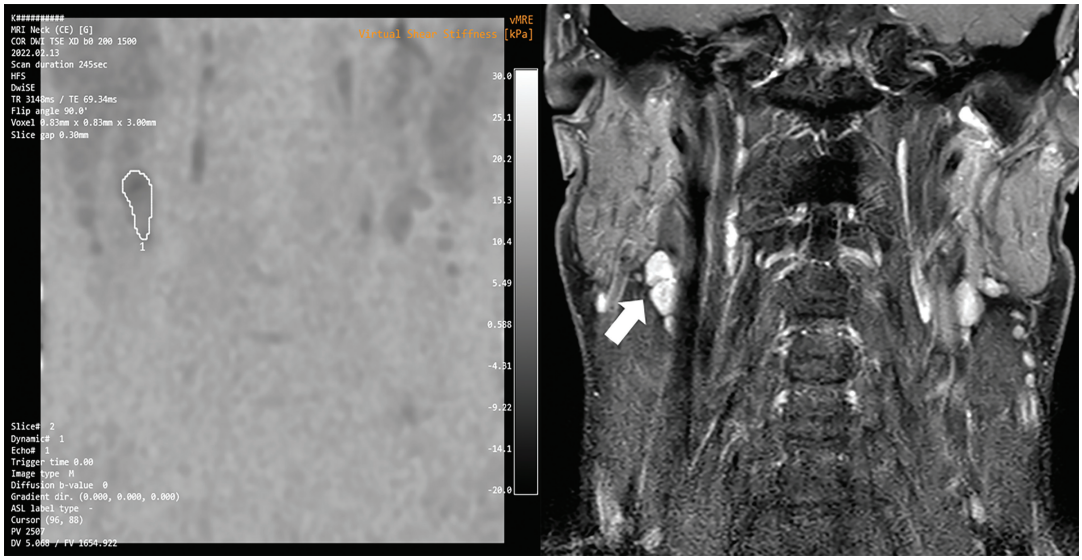


**Fig. 3** A 31-year-old male without any pathology in the neck. An ROI is placed on the largest lymph node at right level II to include whole region of the node on the DWI-based virtual MR elastography map (left side) and contrast-enhanced coronal T1-weighted image shows the right level II lymph node (arrow). DWI, diffusion weighted imaging.

**Table 1** Pathologic diagnoses of 29 cervical lymph nodes

| Pathologic diagnosis | No. of patients | Total No. of lymph nodes |
|---|---|---|
| HNSCC patients | 10 | 16 |
| Oropharynx cancer | 7 | 9 |
| Nasopharynx cancer | 1 | 1 |
| Oral cavity cancer | 1 | 3 |
| Glottis cancer | 1 | 3 |
| Benign patients | 13 | 13 |
| Benign salivary gland tumors | 9 | 9 |
| Pleomorphic adenoma | 5 | 5 |
| Warthin tumor | 4 | 4 |
| Basal cell adenoma | 1 | 1 |
| Schwannoma | 1 | 1 |
| Giant cell granuloma | 1 | 1 |
| None | 1 | 1 |

HNSCC, head and neck squamous cell carcinoma; No., number.

### *Tissue elasticity values of lymph nodes and diagnostic performance of elasticity*

On DWI-based virtual MRE, the mean sADC values of metastatic cervical lymph nodes and benign cervical lymph nodes are 0.551 ± 0.065 ($\times 10^{-3}$ mm$^2$/s, range, 0.438–0.689) and 0.644 ± 0.079 ($\times 10^{-3}$ mm$^2$/s, range, 0.488–0.743), respectively (Table 2). All the elasticity values of metastatic cervical lymph nodes (mean elasticity, 6.86 ± 0.82 kPa; minimum elasticity, 4.95 ± 0.86 kPa; maximum elasticity, 8.6 ± 1.16 kPa; and median elasticity, 6.9 ± 0.9 kPa) were higher than those of benign cervical lymph nodes (mean elasticity, 5.68 ± 0.94 kPa; minimum elasticity, 4.18 ± 1.52 kPa; maximum elasticity, 7.55 ± 0.96 kPa; and median elasticity, 5.74 ± 0.94 kPa). The differences in mean, maximum, and median elasticity values were statistically significant ($P = 0.001$, 0.01, and 0.002 for mean, maximum, and median elasticity, respectively). However, minimum elasticity was not found to be significantly different between the two groups ($P = 0.1$).

In the ROC curve analysis, the areas under the ROC curve (AUCs) of the mean, maximum, and median elasticity values were 0.82, 0.76, and 0.82, respectively. The 95% confidence intervals (CIs) were 0.64–0.94, 0.57–0.9, and 0.64–0.94, respectively. The optimal cutoff values of mean elasticity and median elasticity distinguishing metastatic from benign cervical lymph nodes were 5.83 kPa and 5.97 kPa, respectively. The diagnostic accuracy, sensitivity, specificity, PPV, and NPV of mean elasticity were 82.8%, 93.8%, 69.2%, 78.9%, and 90%, respectively. Diagnostic performances of the elasticity values are listed in Table 3.

One of the 16 metastatic cervical lymph nodes was a false-negative with a mean elasticity value of 5.19 kPa (Fig. 2). Four of the 13 benign cervical lymph nodes were false-positives with mean elasticity values of 6.54, 6.6, 6.61, and 7.6 kPa.

### *Interobserver agreement in measuring the elasticity values*

The mean, minimum, and median elasticity values showed excellent interobserver agreement between the two radiologists

(ICC coefficients for mean, minimum, and median elasticity were 0.98, 0.95, and 0.98, respectively) and maximum elasticity showed moderate interobserver agreement (ICC coefficient = 0.73).

## Discussion

Many recent studies have focused on tissue elasticity using elastography imaging in the evaluation of tumors.[8,10,11,14,17,19] Since the assessment of metastatic cervical lymph nodes in HNSCC is very important in predicting patient prognosis and in determining treatment strategies, numerous studies have investigated different imaging findings or techniques for evaluation in these cases.[1,5,6,12] Some studies have reported on the usefulness of elasticity values of cervical lymph nodes in the evaluation of metastatic cervical lymph nodes using US elastography.[11–14,20]

Here, we evaluated the estimated elasticity values of metastatic cervical lymph nodes from HNSCC and benign cervical lymph nodes on DWI-based virtual MRE. Estimated elasticity values (mean, minimum, and median elasticity) showed excellent interobserver agreement (ICC coefficient, 0.95–0.98). The mean, maximum, and median elasticity values of metastatic cervical lymph nodes showed significantly higher values than those of benign cervical lymph nodes. These elasticity values also showed good diagnostic performance (AUC: 0.76–0.82) in differentiating metastatic cervical lymph nodes of HNSCC from benign cervical lymph nodes.

Our results show much higher interobserver agreement (ICC coefficients, 0.95–0.98) than previous studies based on shear wave US elastography (ICC coefficients, 0.7–0.77).[13,21,22] Besides the intrinsic limitations of subjectivity in US examination, operators usually draw small ROIs in a lymph node on shear wave US elastography due to the heterogeneous nature of US elastography maps. Whereas, we drew ROIs to include the entire region of each lymph node on the DWI-based virtual MRE map, which showed the largest dimension of the lymph node (Figs. 1 and 2). Shear wave US elastography maps are very heterogeneous especially for the neck area that has motion artifacts due to respiration and pulsation of carotid arteries, leading to variable results in case of using small ROIs. Therefore, there is less variability in selecting ROIs in the lymph nodes on DWI-based virtual MRE maps compared with US elastography. However, using 3D ROIs may further increase interobserver agreement and produce more accurate elasticity values of an entire node.

Diagnostic accuracy of elasticity values on DWI-based virtual MRE is shown to be higher than on cross-sectional images (sensitivities less than 75%) and comparable to US elastography.[4–7,11,13,20] However, estimated elasticity values on DWI-based virtual MRE in this study are much lower than those values based on shear wave US elastography. Benign cervical lymph nodes showed a mean elasticity value of 5.68 kPa (range, 4.5–7.6 kPa) compared with 7.8–21.4 kPa in previous studies with shear wave US elastography.[11,13,23,24] The maximum elasticity value of 7.55 kPa (range, 5.86–8.96 kPa) was also lower compared

**Table 2** The sADC values of metastatic cervical lymph nodes and benign cervical lymph nodes

| | sADC values of metastatic lymph nodes ($\times10^{-3}$ mm$^2$/s) | sADC values of benign lymph nodes ($\times10^{-3}$ mm$^2$/s) |
|---|---|---|
| 1 | 0.548 | 0.556 |
| 2 | 0.595 | 0.743 |
| 3 | 0.526 | 0.631 |
| 4 | 0.606 | 0.658 |
| 5 | 0.616 | 0.585 |
| 6 | 0.489 | 0.635 |
| 7 | 0.462 | 0.743 |
| 8 | 0.584 | 0.649 |
| 9 | 0.538 | 0.686 |
| 10 | 0.475 | 0.563 |
| 11 | 0.438 | 0.738 |
| 12 | 0.596 | 0.488 |
| 13 | 0.689 | 0.691 |
| 14 | 0.537 | |
| 15 | 0.558 | |
| 16 | 0.557 | |

sADC, shifted apparent diffusion coefficient.

**Table 3** Diagnostic performance of elasticity values of cervical lymph nodes on DWI-based MR elastography

| Elasticity values | AUC (95% CI) | Diagnostic accuracy (%) | Sensitivity (%) | Specificity (%) | PPV (%) | NPV (%) | *P* value |
|---|---|---|---|---|---|---|---|
| meanMRE | 0.82 (0.64, 0.94) | 82.8 | 93.8 | 69.2 | 78.9 | 90 | <0.001 |
| minMRE | 0.67 (0.47, 0.83) | 72.4 | 93.8 | 46.2 | 71.4 | 87.5 | 0.11 |
| maxMRE | 0.76 (0.57, 0.9) | 75.9 | 62.5 | 84.6 | 83.3 | 64.7 | 0.004 |
| medMRE | 0.82 (0.64, 0.94) | 79.3 | 87.5 | 69.2 | 77.8 | 81.8 | <0.001 |

AUC, area under the receiver operating characteristic curve; DWI, diffusion weighted imaging; maxMRE, maximum MR elasticity; meanMRE, mean MR elasticity; minMRE, minimum MR elasticity; NPV, negative predictive value; PPV, positive predictive value.

to 14.2–20.7 kPa in previous studies.[13,14] For metastatic cervical lymph nodes, our data showed a mean elasticity of 6.86 kPa compared with 22.4–37.1 kPa reported in previous studies with US elastography.[11,13,23] Largely, it might be resulted from the difference of modalities. Previous study reported that US elastography showed higher values than conventional MRE.[25] However, several other factors also affect that. First, US elastography can result in some bias in selecting ROIs, since readers usually draw small ROIs in some portion of a lesion on US elastography maps. Whereas, we drew ROIs including the entire region of each lymph node rather than the small ROIs used on US elastography. Second, DWI-based virtual MRE protocols and calibration parameters are presumed to be another reason for this difference. The DWI-based virtual MRE protocol used in this study was based on liver MRI, and the calibration parameters were also made based on liver parenchymal data.[15–17] A previous study with liver tumors reported that the estimated elasticity values on DWI-based virtual MRE were significantly lower than those on conventional MRE, even though they were well correlated with conventional MRE.[17] They also described that the main reason for the difference could be due to the fact that calibration parameters were set based on liver parenchyma rather than tumor tissue.[17] Therefore, the protocols and calibration parameters of DWI-based virtual MRE were less suitable for the assessment of cervical lymph nodes. Calibration parameters would be different between the parenchyma and tumors, between different tumor types, and even between different organs. It is likely that these parameters can be found in the nature of the lesions, surrounding environments of tissues, and tissue microstructures.

There was one false-negative case and four false-positive cases in this study. The false-negative case with a low elasticity value showed a cervical lymph node with near total necrosis on conventional images (Fig. 2b). Severe necrosis lowered the tissue elasticity values. However, the four false-positive cases in benign cervical lymph nodes showed no significant features themselves. The patient ages (range, 36–75 years) were variable and primary pathologies were variable; two had Warthin tumors, one had a pleomorphic adenoma, and one had a neurogenic tumor in the parapharyngeal space. Pathologic correlation could not be performed since no tissue was obtained from the benign cervical lymph nodes.

There are several limitations to this study. First, the study population is too small to generalize the results. Further studies with a larger population and comparison with conventional imaging findings are warranted to generalize these results. Second, not all of the cervical lymph nodes were proven pathologically. Although all the metastatic cervical lymph nodes were confirmed pathologically, no benign cervical lymph nodes were confirmed. False-positive cases in benign cervical lymph nodes could have some pathology. However, comparison with previous CT scans (examination intervals were 1–9 months in all four patients) showed no significant interval change of the lymph nodes. Third, the key *b* values (200 and 1500 sec/mm$^2$) for calculating sADC on DWI-based virtual MRE were based on liver MRI and calibration parameters were also based on liver parenchyma. Therefore, the calculations were less suitable for the analysis of cervical lymph nodes, which might have led to less accurate values. However, the result that the estimated elasticity values of metastatic lymph nodes on DWI-based virtual MRE were higher than those of benign lymph nodes would remain unchanged. Furthermore, a recent study showed that the elasticity values of pituitary adenomas with those calibration parameters on DWI-based virtual MRE were well correlated with surgical consistency grading.[18] Future studies to determine the optimal *b* values and calibration parameters for cervical lymph nodes by comparing with established elastography methods such as conventional MRE are needed.

## Conclusion

Our study shows that estimated tissue elasticity values of cervical lymph nodes on DWI-based virtual MRE show significant difference between metastatic cervical lymph nodes from HNSCC and benign cervical lymph nodes. Elasticity values of metastatic cervical lymph nodes (mean elasticity = 6.86 $\pm$ 0.82 kPa) show significantly higher values than benign cervical lymph nodes (mean elasticity = 5.68 $\pm$ 0.94 kPa) and present good diagnostic performance (AUC = 0.82, sensitivity = 94%, and specificity = 69%). Furthermore, interobserver agreement in measuring tissue elasticity on DWI-based virtual MRE is excellent (ICC coefficient = 0.98). Elasticity values on DWI-based virtual MRE may be useful for characterizing cervical lymph nodes. The usefulness of elasticity values based on DWI-based virtual MRE should be further evaluated with larger populations and future studies to determine the optimal calibration parameters and MR protocols specific for analysis of cervical lymph nodes are recommended.

## Conflicts of Interest

The authors declare that they have no conflicts of interest.

## References

1. Ahuja AT, Ying M, Ho SY, et al. Ultrasound of malignant cervical lymph nodes. Cancer Imaging 2008; 8:48–56.
2. Vassallo P, Edel G, Roos N, Naguib A, Peters PE. In-vitro high-resolution ultrasonography of benign and malignant lymph nodes. A sonographic-pathologic correlation. Invest Radiol 1993; 28:698–705.
3. Pritzker KPH, Nieminen HJ. Needle biopsy adequacy in the era of precision medicine and value-based health care. Arch Pathol Lab Med 2019; 143:1399–1415.
4. Castelijns JA, van den Brekel MW. Imaging of lymphadenopathy in the neck. Eur Radiol 2002; 12:727–738.

5. Curtin HD, Ishwaran H, Mancuso AA, Dalley RW, Caudry DJ, McNeil BJ. Comparison of CT and MR imaging in staging of neck metastases. Radiology 1998; 207:123–130.
6. Holzapfel K, Duetsch S, Fauser C, Eiber M, Rummeny EJ, Gaa J. Value of diffusion-weighted MR imaging in the differentiation between benign and malignant cervical lymph nodes. Eur J Radiol 2009; 72:381–387.
7. van den Brekel MW, van der Waal I, Meijer CJ, Freeman JL, Castelijns JA, Snow GB. The incidence of micrometastases in neck dissection specimens obtained from elective neck dissections. Laryngoscope 1996; 106:987–991.
8. Hennedige TP, Hallinan JT, Leung FP, et al. Comparison of magnetic resonance elastography and diffusion-weighted imaging for differentiating benign and malignant liver lesions. Eur Radiol 2016; 26:398–406.
9. Jain RK. Barriers to drug delivery in solid tumors. Sci Am 1994; 271:58–65.
10. Jamin Y, Boult JKR, Li J, et al. Exploring the biomechanical properties of brain malignancies and their pathologic determinants in vivo with magnetic resonance elastography. Cancer Res 2015; 75:1216–1224.
11. Bhatia KS, Cho CC, Tong CS, Yuen EH, Ahuja AT. Shear wave elasticity imaging of cervical lymph nodes. Ultrasound Med Biol 2012; 38:195–201.
12. Che D, Zhou X, Sun ML, Wang X, Jiang Z, Changjun-Wu. Differentiation of metastatic cervical lymph nodes with ultrasound elastography by virtual touch tissue imaging: preliminary study. J Ultrasound Med 2015; 34:37–42.
13. Chen BB, Li J, Guan Y, et al. The value of shear wave elastography in predicting for undiagnosed small cervical lymph node metastasis in nasopharyngeal carcinoma: a preliminary study. Eur J Radiol 2018; 103:19–24.
14. Choi YJ, Lee JH, Lim HK, et al. Quantitative shear wave elastography in the evaluation of metastatic cervical lymph nodes. Ultrasound Med Biol 2013; 39:935–940.
15. Kromrey ML, Le Bihan D, Ichikawa S, Motosugi U. Diffusion-weighted MRI-based virtual elastography for the assessment of liver fibrosis. Radiology 2020; 295:127–135.
16. Le Bihan D, Ichikawa S, Motosugi U. Diffusion and intravoxel incoherent motion MR imaging-based virtual elastography: a hypothesis-generating study in the liver. Radiology 2017; 285:609–619.
17. Ota T, Hori M, Le Bihan D, et al. Diffusion-based virtual MR elastography of the liver: can it be extended beyond liver fibrosis? J Clin Med 2021; 10:4553.
18. Lagerstrand K, Gaedes N, Eriksson S, et al. Virtual magnetic resonance elastography has the feasibility to evaluate preoperative pituitary adenoma consistency. Pituitary 2021; 24:530–541.
19. Lee SH, Chang JM, Kim WH, et al. Differentiation of benign from malignant solid breast masses: comparison of two-dimensional and three-dimensional shear-wave elastography. Eur Radiol 2013; 23:1015–1026.
20. Ghajarzadeh M, Mohammadifar M, Azarkhish K, Emami-Razavi SH. Sono-elastography for differentiating benign and malignant cervical lymph nodes: a systematic review and meta-analysis. Int J Prev Med 2014; 5:1521–1528.
21. Bhatia K, Tong CS, Cho CC, Yuen EH, Lee J, Ahuja AT. Reliability of shear wave ultrasound elastography for neck lesions identified in routine clinical practice. Ultraschall Med 2012; 33:463–468.
22. Choi YJ, Lee JH, Baek JH. Ultrasound elastography for evaluation of cervical lymph nodes. Ultrasonography 2015; 34:157–164.
23. Kim HJ, Choi IH, Jin SY, et al. Efficacy of shear-wave elastography for detecting postoperative cervical lymph node metastasis in papillary thyroid carcinoma. Int J Endocrinol 2018; 2018:9382649.
24. Qin Q, Wang D, Xu L, Lan Y, Tong M. Evaluating lymph node stiffness to differentiate bacterial cervical lymphadenitis and lymph node-first presentation of kawasaki disease by shear wave elastography. J Ultrasound Med 2021; 40:1371–1380.
25. Imajo K, Honda Y, Kobayashi T, Nagai K, Ozaki A, Iwaki M, et al. Direct comparison of US and MR elastography for staging liver fibrosis in patients with nonalcoholic fatty liver disease. Clin Gastroenterol Hepatol. 2022; 20:908–917.e11.